International Journal of Scientific and Technological Research www.iiste.org
ISSN 2422-8702 (Online), **DOI:** 10.7176/JSTR/5-4-12
Vol.5, No.4, 2019

Dependence of Inhibition Effects of Oxalate, Tungstate, Molybdate and Phosphate on Purity of Zinc Metal

T. Yanardag (Corresponding author),
Department of Chemistry Faculty of Science,
University of Ankara, 06100 Tandogan, Dogol St. Ankara, Turkey

M. Kuyukoglu
Department of Chemistry Faculty of Science,
University of Ankara, 06100 Tandogan, Dogol St. Ankara, Turkey

A.A. Aksut
Department of Chemistry Faculty of Science,
University of Ankara, 06100 Tandogan, Dogol St. Ankara, Turkey

Abstract
The inhibition effects of oxalate, tungstate, molybdate and phosphate on corrosion of 99.99 %, 99.999 % zinc and 99.95 % molybdenum metals were investigated in NaCl solutions by potential-time, AC-impedance spectra and current-potential curves. The corrosion rates of metals are highly dependent on the purity of its. The inhibition effect of these anions on 99.999 % purity zinc is less than the effect on 99.99 % purity zinc. This implies that alloying elements are effective on inhibiting efficiencies of these anions. Inhibition effect of these anions decreases also with increasing NaCl concentration. None of the studied anions behaved as inhibitors on 99.999 % purity zinc in 1 M NaCl solution. The corrosion mechanism on the zinc metals is charge-transfer, but reaction on the molybdenium is diffusion controlled in the studied solutions.

Keywords: Zinc, corrosion, oxalate, tungstate, molybdate, phosphate

DOI: 10.7176/JSTR/5-4-12

1. Introduction

Zinc is most commonly used as an alloying element and for cathodic protection [1-3]. Its standard electrode potential is -0.76 V (vs. SHE), for this reason, it is susceptible to the corrosion. Due to its high reactivity, zinc metal and its alloys must be protected against corrosion [4]. The corrosiveness of the media can be decreased by adding various inhibitors [5-8]. It is important that the inhibitors to be used must not be toxic as chromate and nitrate [9]. In recent studies, the inhibition effect of inorganic onions such as $C_2O_4^{-2}$, MoO_4^{-2}, WO_4^{-2} and HPO_4^{-2} have been investigated on the corrosion of zinc, zinc alloys and some other metals [10-15, 19].

Oxalate ions were found to be an effective inhibitor in our previous studies on magnesium, zinc, copper and brass especially in NaCl solutions [16-19]. This effect decreases with increasing concentration of $C_2O_4^{-2}$ and the most effective concentration was observed to be 10^{-3} M [17]. In this study, the effects of MoO_4^{-2}, WO_4^{-2}, HPO_4^{-2} and $C_2O_4^{-2}$ on the corrosion 99.99 % and 99.999 % pure zinc metals in neutral solutions were investigated by using electrochemical methods. Inhibition effect of $C_2O_4^{-2}$ was decreased with increasing $C_2O_4^{-2}$ concentration. ZnC_2O_4 formed on the metal surface reacts with $C_2O_4^{-2}$ .At the high $C_2O_4^{-2}$ concentration dissolves it, just as the dissolution of $Zn(OH)_2$ on the metal surface at high concentrations of OH^-.For this reason, inhibition effect of $C_2O_4^{-2}$ on zinc was decreased at the high $C_2O_4^{-2}$ concentration[19,20]. The effect of minor impurities in zinc metals was also observed on the inhibition effects of the anions used for corrosion protection of zinc. Furthermore, Cl^- ion concentration in the studied medium was effective on the metal corrosion and inhibition effect of studied anions as inhibitor. At the higher Cl^- concentration was not observed any inhibition effect of these inorganic anions on the corrosion of 99.999 % purity zinc.

ISSN 2422-8702 (Online), **DOI:** 10.7176/JSTR/5-4-12
Vol.5, No.4, 2019

2. Experimental

A cylinder pure zinc rod (Aldrich, 99.999 %, 2 mm diameter and 99.99 % purity, 5 mm diameter) and molybdenum (Aldrich, 99.95 % purity, 5 mm diameter) were fixed in the teflon tube with adhesive. The working electrode was polished with 1200 grid emery papers and washed with double distilled water before each experiment. The potential-time (20 minutes), current-potential (1mV/s) and AC-impedance curves were obtained by an electrochemical system of a CH-Instruments 660B Potentiostat, an electrochemical work station of computer programme, a BAS disc electrode, and a Poly Science model 9106 thermostat. Saturated Ag/AgCl electrode and a platinum wire were used as reference and counter electrodes, respectively. The impedance measurements were performed at the open circuit potential of working electrode with voltage perturbation amplitude of 5 mV in a frequency range between 10^5-0.1 Hz. Corrosion rates, polarization resistances and other corrosion characteristics of pure zinc and molybdenum metals were obtained in 0.5 M and 1 M NaCl solutions containing $Na_2C_2O_4$, Na_2WO_4, Na_2MoO_4 and Na_2HPO_4. All chemicals used are Merck grade. Corrosive media were prepared with double distilled water. All measurements were carried out in aerated solution at 25°C. The working electrodes were immersed 20 seconds in 0.15 M HCl solution and then washed with double distilled water for obtaining better electrode surface before immersing in the corrosive solutions [22, 23].

3. Results and discussion

The potential-time and AC-impedance diagrams of 99.999 % and 99.99 % pure zinc metals obtained in 0.5 M NaCl solutions containing oxalate, molybdate, tungstate and phosphate are shown in Figures 1-2. The corrosion characteristics of metals calculated using these and potential-current curves are given in Tables 1-2. The potential-time and AC-impedance diagrams of 99.999 % and 99.99 % zinc metal obtained in 1 M NaCl solutions are given in Figure 3-5 and the corrosion characteristics are given in Table 3-4. The previous studies were showed that 10^{-3} M concentration of the inorganic compounds was sufficient for high inhibition rates. For this reason, 10^{-3} M inhibitor concentration was used in this study [17]. None of the studied anions behaved as inhibitors on 99.999 % purity zinc in 1 M NaCl solution.

As the purity of zinc metal increases, the inhibition decreases and is totally eliminated for oxalate as can be seen in Tables 1 and 2. This shows that corrosion protection of zinc, zinc alloys and zinc coated metals with oxalate does not originate from the zinc metal itself. Experiments in 1 M NaCl solutions containing 10^{-2} M and 10^{-1} M $C_2O_4^{-2}$ were performed in order to see the effect of increasing oxalate concentration on the corrosion of 99.999 % zinc. If $C_2O_4^{-2}$ concentration is too low, solid ZnC_2O_4 formed on the metal surface and acts as a protective layer. As $C_2O_4^{-2}$ concentration increases, inhibition decreases. Inhibition effect disappears for 99.99 % zinc in 0.5 M NaCl solution containing 10^{-1} M oxalate (Table 2) and for 99.999 % zinc in 1 M NaCl solution containing 10^{-2} M oxalate (Table 3). This strengthens idea that solid ZnC_2O_4 dissolves in the form of $Zn(C_2O_4)_2^{-2}$ in the presence of excess $C_2O_4^{-2}$ ions according to the reaction shown below.

$$ZnC_2O_{4(k)} + C_2O_{4(aq)}^{2} \rightarrow Zn(C_2O_4)_{2(aq)}^{2}$$

The corrosion rate of 99.999 % pure zinc accelerates with increasing NaCl concentration (Tables 1 and 3). Adsorption of Cl^- on the metal surface increased and this adsorbed layer Cl^- prevents adsorption of $C_2O_4^{-2}$, MoO_4^{-2}, WO_4^{-2} and HPO_4^{-2}. For this reason, ZnC_2O_4, $ZnMoO_4$, $ZnWO_4$ and $ZnHPO_4$ are not formed on the metals surface and protection against corrosion cannot be observed.

In general, potential-time curves show that corrosion rate increases when the open circuit potential of metal shifts in the negative direction and corrosion decreased with the shift to the positive direction with surface covering by corrosion products. According to the latest potential readings in Figure 1 (99.999 % zinc), the open circuit potential of only $C_2O_4^{-2}$ containing medium is more negative than that of NaCl medium and oxalate is not acted as inhibitor in this medium (Table 1).Corrosion potentials are more positive than NaCl solution, if the solution containing molybdate, tungstate and phosphate.and under these conditions, molybdate, tungstate and phosphate act as anodic inhibitors. Open circuit potentials of 99.99 % pure zinc in 0.5 M NaCl solutions containing oxalate, molybdate and tungstate shift positive and they act as anodic inhibition The potential shifts in the negative direction in 0.5M NaCl solution containing phosphate(Table 2).For this reason, phosphate acts as cathodic inhibitor. From AC-impedance diagrams, it can be revealed that corrosion occurs by a charge transfer mechanism in all solutions other than HPO_4^{-2} containing solution. Nyquist diagrammes are semicircle. The impedance values increases with the increasing inhibition efficiencies. These results are consistent with the corrosion rates determined from current-potential curves (Table 1). The same situation is observed for 99.99 % zinc in

ISSN 2422-8702 (Online), **DOI:** 10.7176/JSTR/5-4-12
Vol.5, No.4, 2019

0.5 M NaCl solution (Figures 2 and Table 2). These results show that corrosion under these conditions occurs as a charge transfer controlled process.

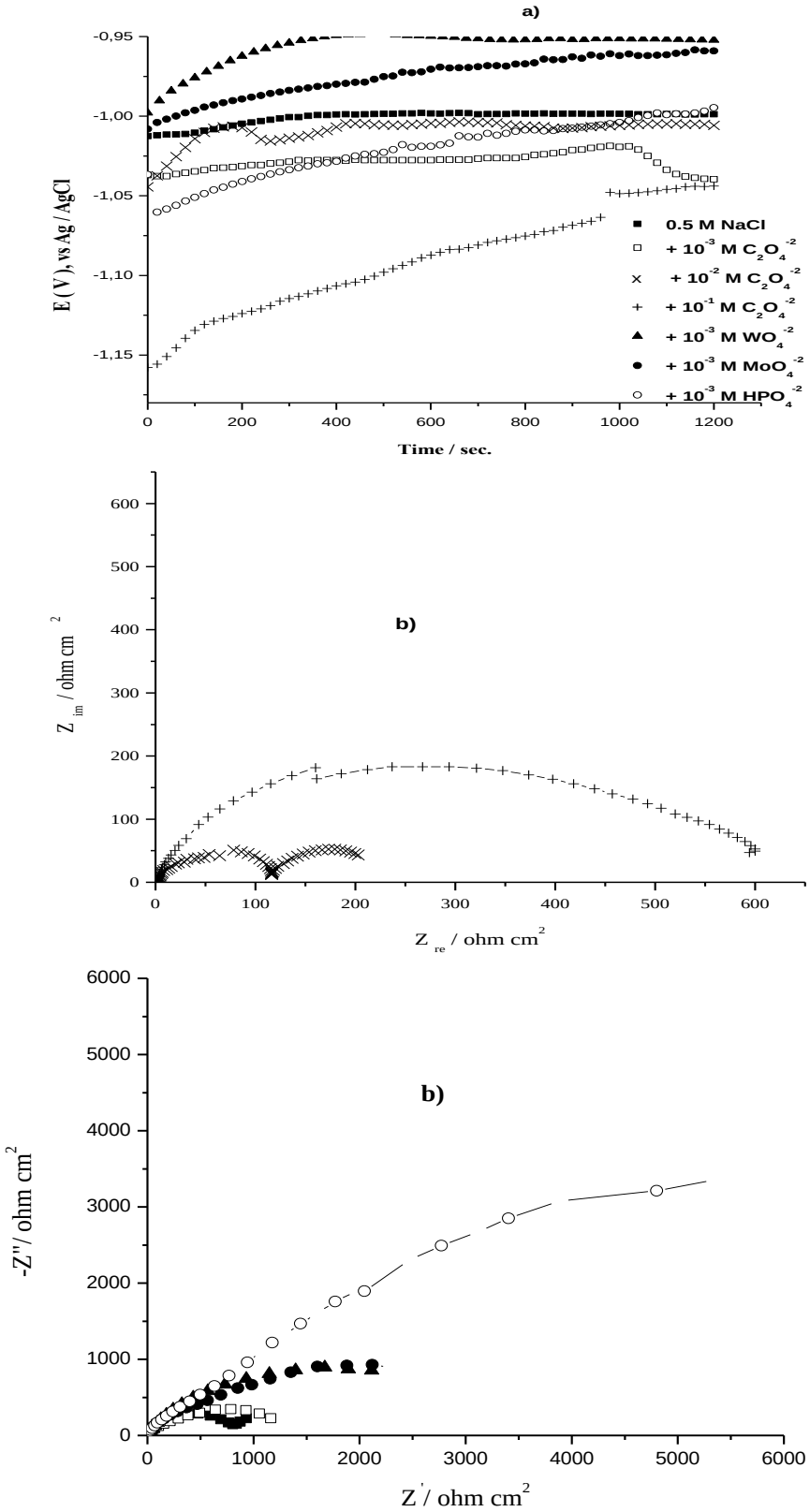

Figure 1. a) potential-time and b) impedance curves of 99.999 % purity zinc in 0.5 M NaCl + 10^{-3} M x [x: 0 (■) , $C_2O_4^{2-}$ (□), WO_4^{2-} (▲), MoO_4^{2-} (●) and HPO_4^{2-} (○)] and 0.5 M NaCl + x M $C_2O_4^{2-}$ [x: 10^{-2} (x) , 10^{-1} (+)] solutions at 25°C

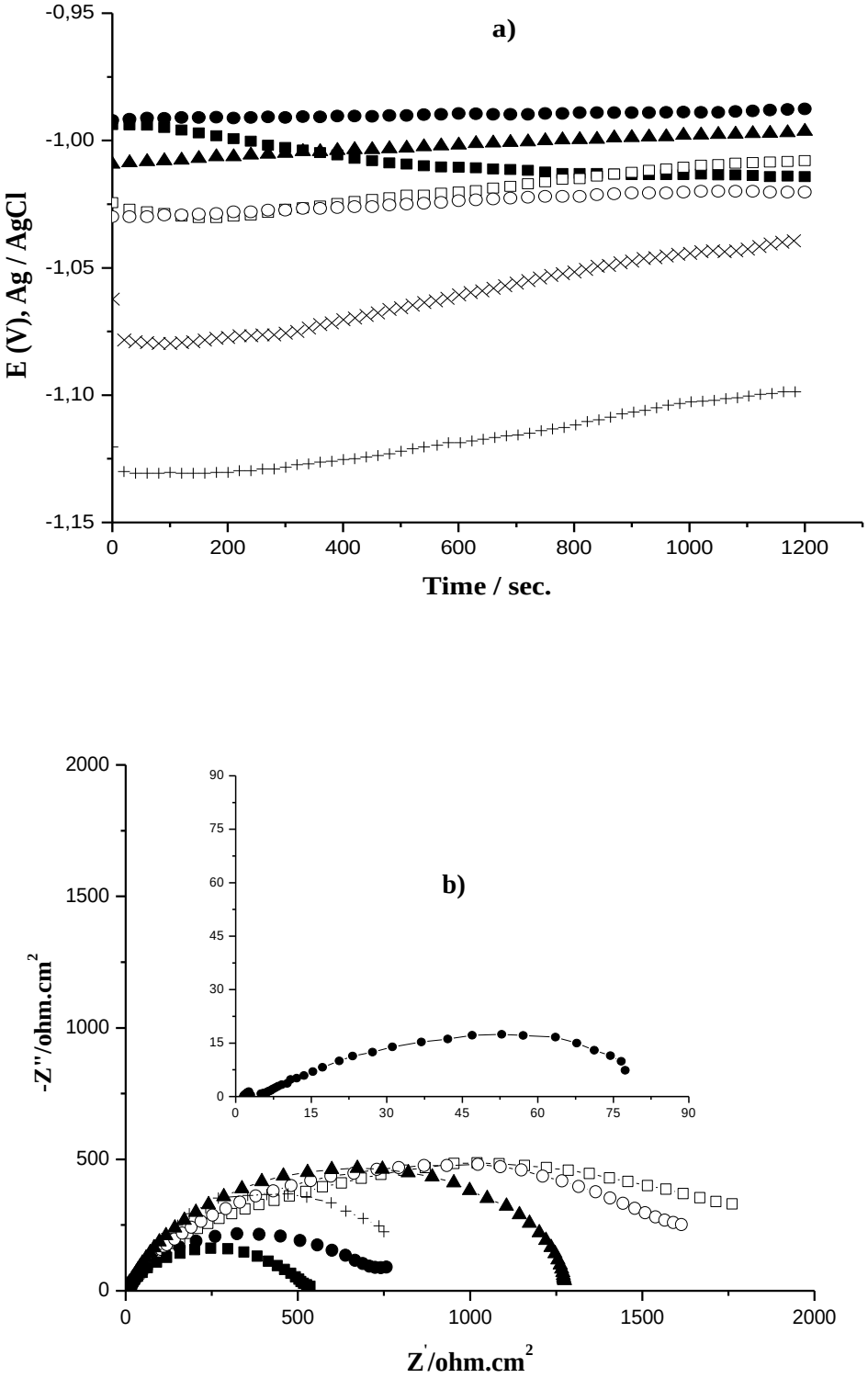

Figure 2. a) potential-time and b) impedance curves of 99.99 % purity zinc in 0.5 M NaCl + 10^{-3} M x [x: 0 (■) , $C_2O_4^{2-}$ (□), WO_4^{2-} (▲), MoO_4^{2-} (●) and HPO_4^{2-} (○)] and 0.5 M NaCl + x M $C_2O_4^{2-}$ [x: 10^{-2} (x) , 10^{-1} (+)] solutions at 25°C

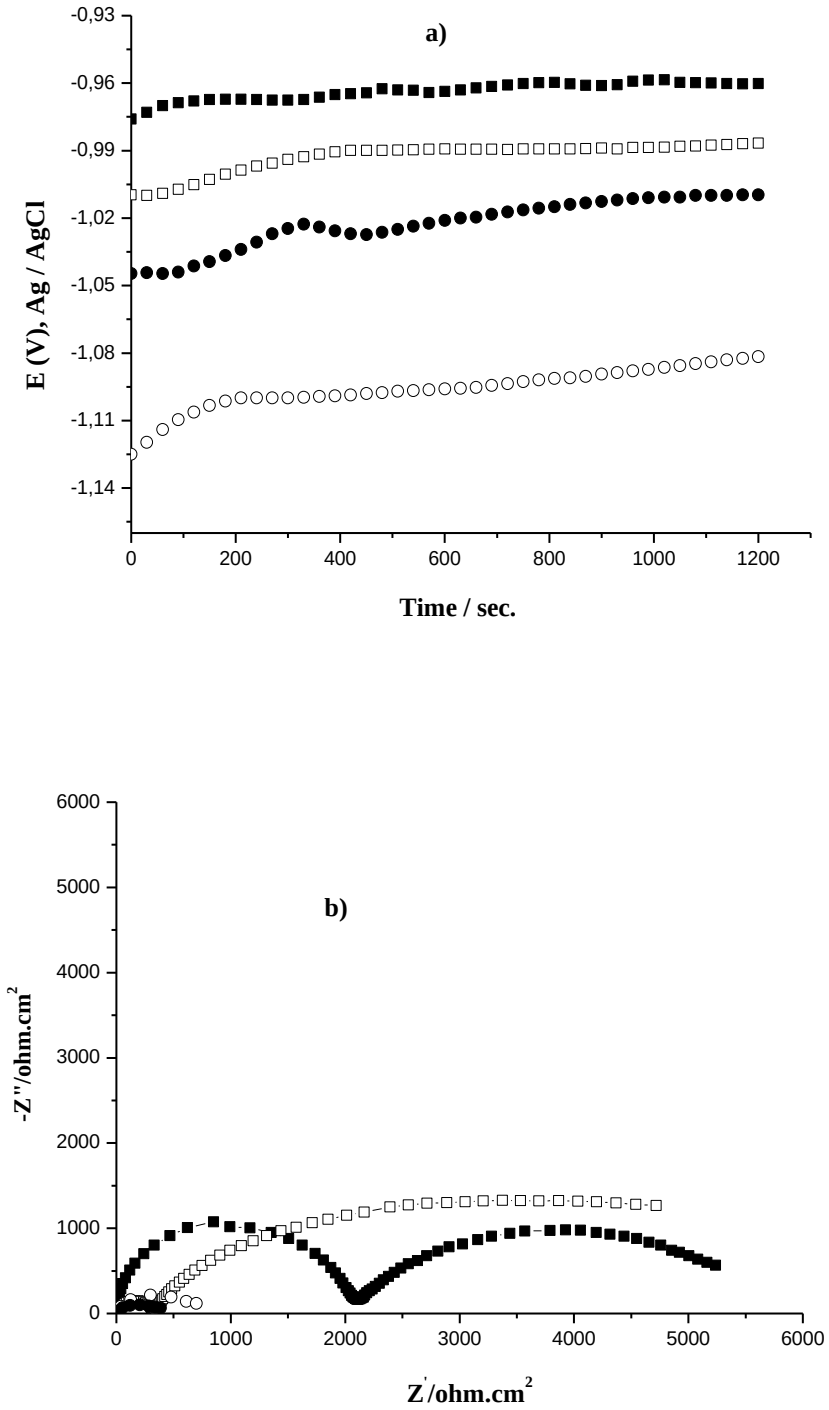

Figure 3. a) potential-time and b) impedance curves of 99.999 % purity zinc in 1 M NaCl + 10^{-3} M x [x: 0 (■) , $C_2O_4^{2-}$ (□), WO_4^{2-} (▲), MoO_4^{2-} (●) and HPO_4^{2-} (○)] solutions at 25°C

ISSN 2422-8702 (Online), **DOI:** 10.7176/JSTR/5-4-12
Vol.5, No.4, 2019

Table 1. The corrosion characteristics of 99.999 % pure zinc obtained in 0.5 M NaCl solution containing $C_2O_4^{2-}$, WO_4^{2-}, MoO_4^{2-} and HPO_4^{2-} at 25°C

Solution	E_{corr} (V) vs. Ag/AgCl	$-b_c$ (mV dec^{-1})	b_a (mV dec^{-1})	R_p (Ω cm^2)	C_{dl} (F cm^{-2})	i_{corr} (μA cm^{-2})	% η
Blank	-1.026	141	153	3926	2.1×10^{-7}	6.0	
$+10^{-3}$ M $C_2O_4^{2-}$	-1.088	162	66	1880	3.7×10^{-7}	10.2	-
$+10^{-2}$ M $C_2O_4^{2-}$	-1.020	284	86	1669	2.7×10^{-6}	45	-
$+10^{-1}$ M $C_2O_4^{2-}$	-1.203	58.8	367	466	2.8×10^{-6}	77.7	-
$+10^{-3}$ M WO_4^{2-}	-1.028	204	48	12495	2.2×10^{-8}	1.1	82
$+10^{-3}$ M MoO_4^{2-}	-1.053	260	62	9792	2.6×10^{-8}	2.6	57
$+10^{-3}$ M HPO_4^{2-}	-1.074	255	62	16341	4.3×10^{-9}	2.4	60

Table 2. The corrosion characteristics of 99.99 % purity zinc obtained in 0.5 M NaCl and $C_2O_4^{2-}$, WO_4^{2-}, MoO_4^{2-} and HPO_4^{2-} containing 0.5 M NaCl solutions at 25°C.

Solution	E_{corr} (V) vs. Ag/AgCl	$-b_c$ (mV dec^{-1})	b_a (mV dec^{-1})	R_p (Ω cm^2)	C_{dl} (F cm^{-2})	i_{corr} (μA cm^{-2})	% η
Blank	-1.06	334	70	736	$8.95\text{x}10^{-6}$	33.9	
$+10^{-1}$ M $C_2O_4^{2-}$	-1.233	173	175	913	$4.27\ \text{x}10^{-3}$	42.1	-
$+10^{-2}$ M $C_2O_4^{2-}$	-1.123	209	51	1231	$1.53\ \text{x}10^{-4}$	14.5	57
$+10^{-3}$ M $C_2O_4^{2-}$	-1.036	312	71	2082	$5.01\text{x}10^{-7}$	15.0	56
$+10^{-3}$ M WO_4^{2-}	-1.047	337	44	4003	$1.89\ \text{x}10^{-5}$	4.4	87
$+10^{-3}$ M MoO_4^{2-}	-1.021	200	43	3933	$1.76\ \text{x}10^{-5}$	5.0	85
$+10^{-3}$ M HPO_4^{2-}	-1.155	202	56	9904	$4.93\ \text{x}10^{-5}$	3.4	90

Table 3. The corrosion characteristics of 99.999 % purity zinc obtained in 1 M NaCl solutions containing $C_2O_4^{2-}$, WO_4^{2-}, MoO_4^{2-} and HPO_4^{2-} at 25°C

Solution	E_{corr} (V) vs. Ag/AgCl	$-b_c$ (mV dec^{-1})	b_a (mV dec^{-1})	R_p (Ω cm^2)	C_{dl} (F cm^{-2})	i_{corr} (μA cm^{-2})	% η
Blank	-1.023	252.4	164.9	17063	1.3×10^{-8}	3.68	
$+10^{-3}$ M $C_2O_4^{2-}$	-1.045	190.1	142.2	19942	9.0×10^{-9}	4.50	-
$+10^{-2}$ M $C_2O_4^{2-}$	-1.144	111.0	47.6	1494	1.5×10^{-6}	9.79	-
$+10^{-1}$ M $C_2O_4^{2-}$	-1.205	143.9	265.3	687	1.6×10^{-6}	61.1	-
$+10^{-3}$ M WO_4^{2-}	-1.044	244.8	45.0	1392	7.9×10^{-7}	11.8	-
$+10^{-3}$ M MoO_4^{2-}	-1.068	248.7	46.3	2153	4.0×10^{-7}	7.76	-
$+10^{-3}$ M HPO_4^{2-}	-1.129	133.0	66.5	2931	2.3×10^{-7}	7.12	-

ISSN 2422-8702 (Online), **DOI:** 10.7176/JSTR/5-4-12
Vol.5, No.4, 2019

The open-circuit potential of 99.999 % zinc metal measured in 1 M NaCl solution is more positive than $C_2O_4^{-2}$, MoO_4^{-2}, WO_4^{-2} and HPO_4^{-2} containing conditions, and there is no inhibition observed in this case (Figures 3a and 4a). The corrosion process is also charge transfer controlled in this condition (Figure 3b and 4b). The polarization resistance (Rp) decreases by the addition of inorganic anions to the solution (Table 3).The impedance diagrams obtained in 1 M NaCl solution appear in the form of two consecutive semi-circles, implying the existence double layer. (Figures 3b).

The impedance diagrams obtained for %99.99 zinc in 1 M NaCl solution appear one semi-circle (Figure 5b). The layer at the high frequency region becomes thinner by addition of $C_2O_4^{-2}$ to the medium. Corrosion characteristics obtained with %99.99 zinc in 1 M NaCl are given in Table 4. In recent studies, it is stated that $Zn(OH)_2$ dissolves in the form of $Zn(OH)_3^-$ in high pH solutions where an excess of OH^- exists and CuCl dissolves in the form $CuCl_2^-$ [19,20,23]. Two anodic current peaks was observed at the current-potential curves .The first current peak potential related to the formation of zinc hydroxide is -1.15 V and the second current peak indicate the conversion of $Zn(OH)_2$ to $Zn(OH)_3^-$ by the reaction at the below is -1.00 V (vs. Ag/AgCl).

$$Zn(OH)_2 + 3OH^- \rightarrow Zn(OH)_3^-$$

Similar situation is observed for %99.999 purity zinc at the higher $C_2O_4^{-2}$ concentration (Figure 4c). A second anodic current peak observed in current-potential curves can be shows dissolving ZnC_2O_4 to the $Zn(C_2O_4)_2^{-2}$ by the equation below (Figure 4c). First current peak was observed at -1.14 V and second current peak was observed at -1.0V. Under these conditions, the corrosion rates determined are higher and the inhibition efficiency is low (Table 3).

$$ZnC_2O_4\,(solid) + 2e^- \rightarrow ZnC_2O_2^{-2}$$

These anodic current peaks can be also show formation of Zn^+ and Zn^{+2} ions according to the reactions below.

$$Zn + C_2O_4^{-2}\,(ads.) \rightarrow ZnC_2O_4^-(ads.) + e^-$$

$$ZnC_2O_4^-(ads.) \rightarrow ZnC_2O_4(solid) + e^-$$

ISSN 2422-8702 (Online), **DOI:** 10.7176/JSTR/5-4-12
Vol.5, No.4, 2019

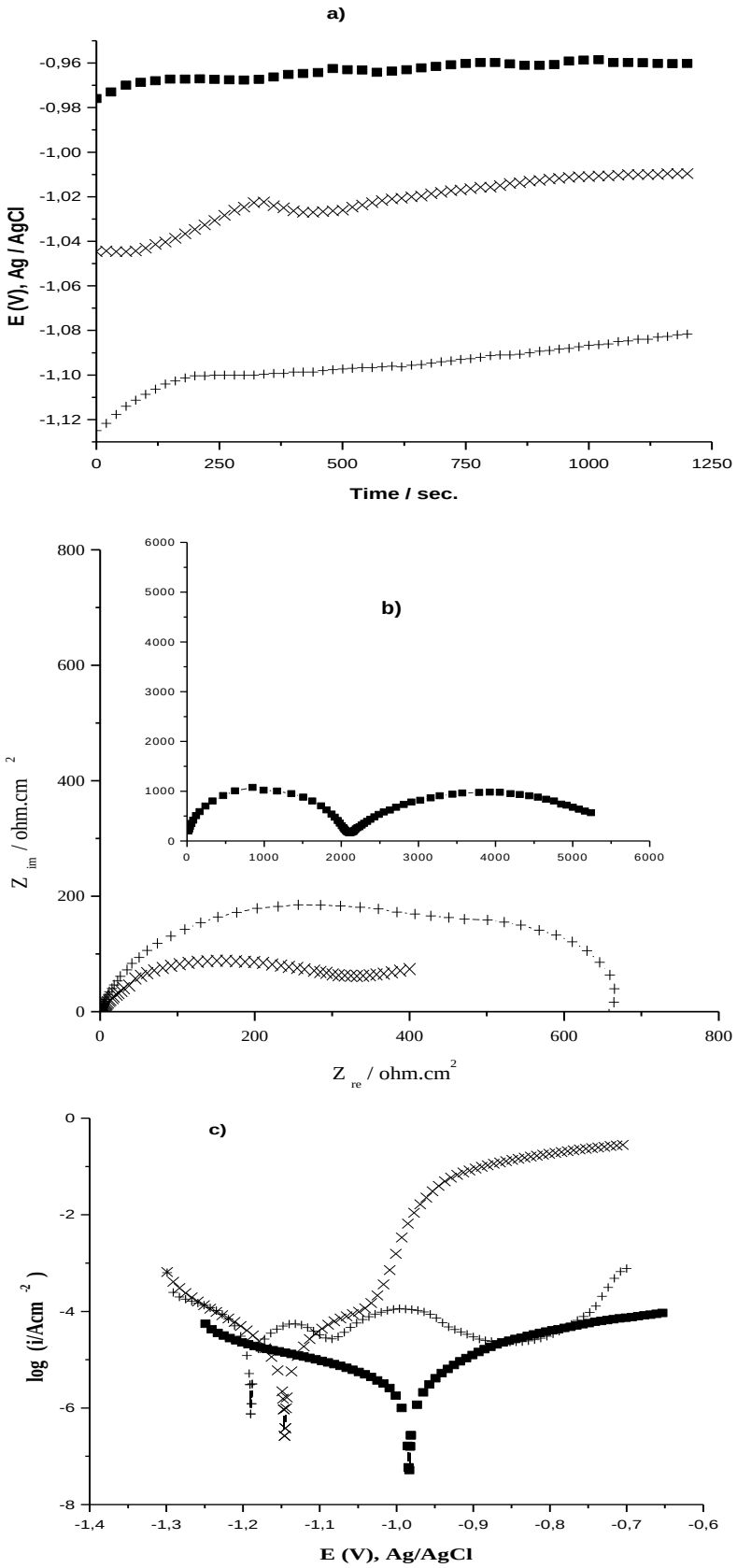

Figure 4. a) potential-time and b) impedance and c) current-potential curves of 99.999 % purity zinc in 1 M NaCl + x M $C_2O_4^{2-}$ [x: 10^{-2} M (x) and 10^{-1} M (+)] solutions at 25°C

ISSN 2422-8702 (Online), **DOI:** 10.7176/JSTR/5-4-12
Vol.5, No.4, 2019

These results can be show that Zn^{+} ion forms at the -1.14 V and Zn^{+2} ion forms at the -1.0 V on the %99.999 purity zinc in 1M NaCl + 10^{-1} M $C_2O_4^{-2}$ solution at 25° C. Impurity in zinc metal albeit a very small amount affects the effectiveness of the inhibitor. The increasing in inhibition effect of $C_2O_4^{-2}$ with the increasing in impurities, indicate that the inhibition effect of oxalate on zinc metal also depends on the alloying elements of the metal. The most abundant alloying element in the less pure metal is molybdenum, and it is found that oxalate inhibits the corrosion of this metal in 0.5 M NaCl solution (Tables 5). This shows that molybdenum has positive influence on the inhibition effect of $C_2O_4^{-2}$. The conductivity of the layer formed on the molybdenum metal surface is very small and the corrosion occurs by a diffusion controlled mechanism [24]. The magnitude of the observed impedance values confirmed this (Table 5 and Figure 6). In order to observe the effect of pH on the inhibition effect of $C_2O_4^{-2}$ on the corrosion of molybdenum, potential-time, current-potential and AC-impedance curves were obtained also in 0.5M HCl and 0.49M NaCl + 0.01M NaCl solutions (Figures 7 and 8). The corrosion characteristics determined from these curves are given in Tables 6. The inhibition effect of oxalate is slightly increased in basic solution, while inhibition is not observed in acidic solution. This implies that $Mo_2(C_2O_4)_3$ is not formed, instead $H_2C_2O_4$ is formed in acidic medium as shown below.

$$C_2O_4^{-2} + 2H^{+} \rightarrow H_2C_2O_4$$

The formation of $Mo_2(C_2O_4)_3$ both depends on the concentrations of Mo^{+3} and $C_2O_4^{-2}$ where the reaction may occur as given below.

$$Mo^{+3} + C_2O_4^{-2} \rightarrow MoC_2O_4^{+}$$

$$2Mo^{+3} + 3C_2O_4^{-2} \rightarrow Mo_2(C_2O_4)_3$$

If the concentrations both Mo^{+3} ion and $C_2O_4^{-2}$ ion are low, the reaction leading to the formation of $MoC_2O_4^{+}$ will occur. $Mo_2(C_2O_4)_3$ will be produced in the case of high concentrations of both reactants. If there is no $C_2O_4^{-2}$ ions in the solution, MoO_2 (-0.070 V vs. SHE) or Mo^{+3} (-0.200 V vs. SHE) will form on the metal surface [25]. The equilibrium potentials in Tables 5 and 6 indicate that MoO_2 or Mo^{+3} may be produced.

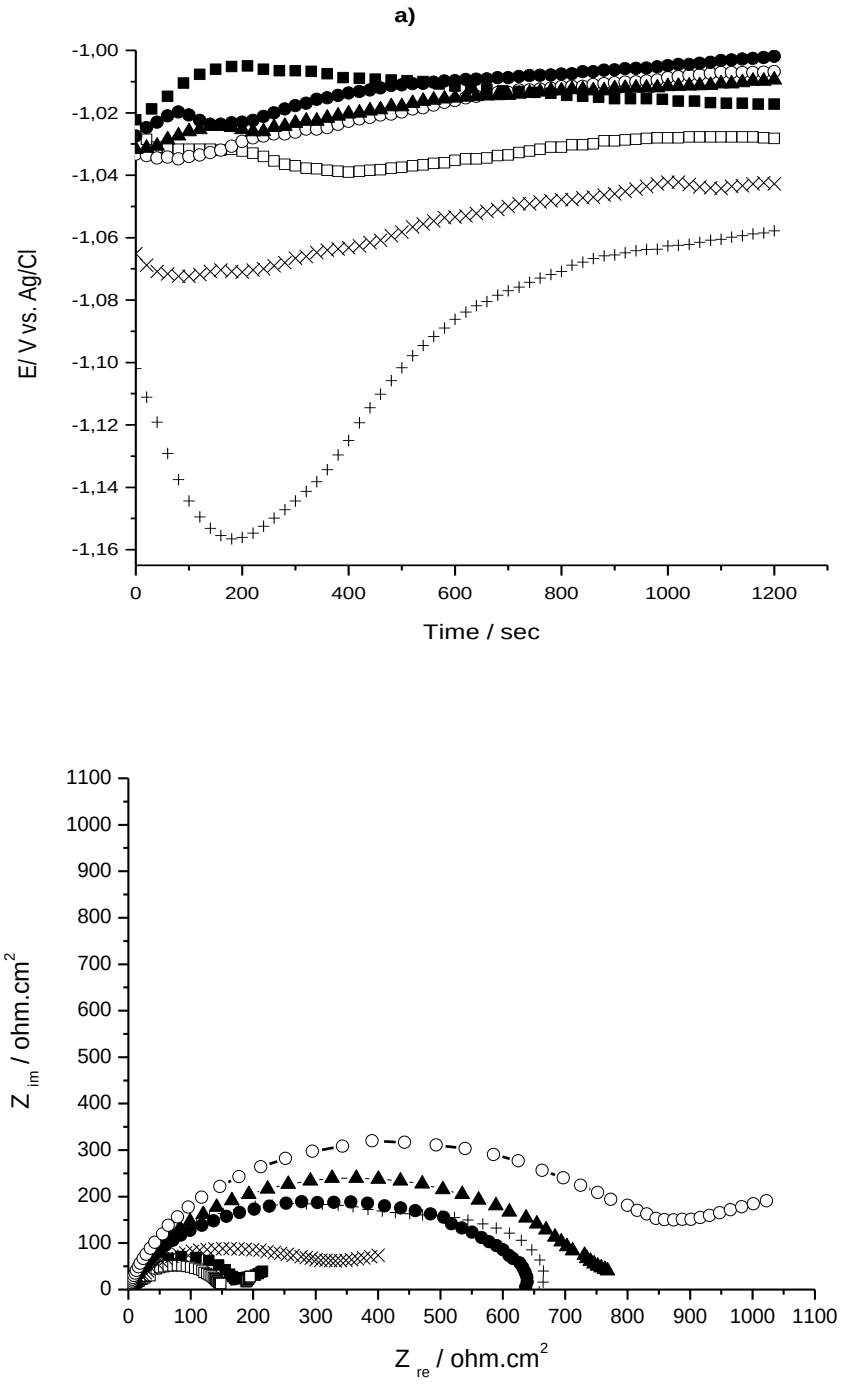

Figure 5. a) potential-time and b) impedance curves of 99.99 % purity zinc in 1 M NaCl + 10^{-3} M x [x: 0 (■) , $C_2O_4^{2-}$ (□), WO_4^{2-} (▲), MoO_4^{2-} (●) and HPO_4^{2-} (○)] and 1 M NaCl + x M $C_2O_4^{2-}$ [x: 10^{-2} (x) , 10^{-1} (+)] solutions at 25°C

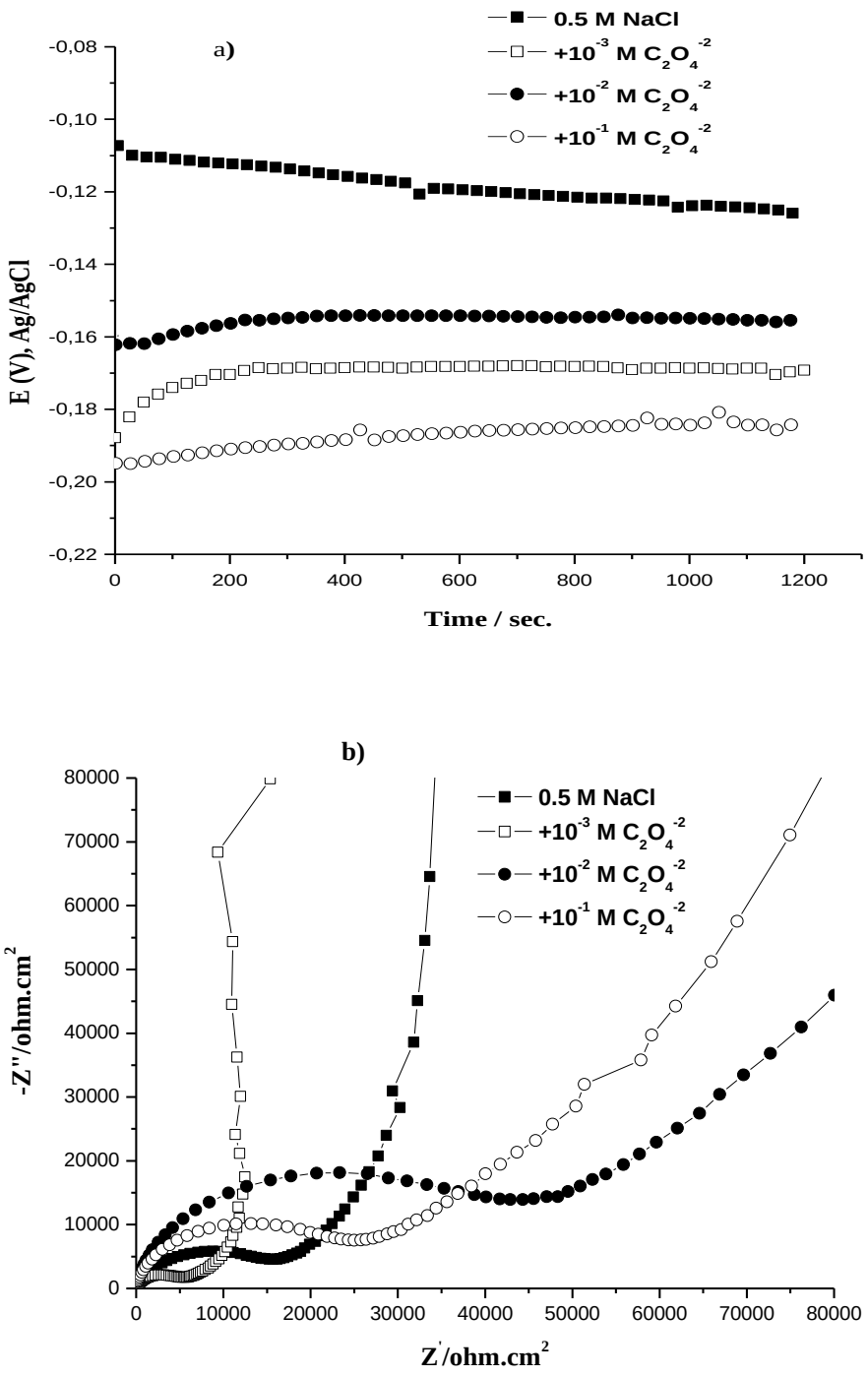

Figure 6. a) potential-time and b) impedance curves of 99.95 % purity molybdenum in 0.5 M NaCl + x M $C_2O_4^{2-}$ [x: 0 (■), 10^{-3} M (□), 10^{-2} M (●) and 10^{-1} M (○)] solutions at 25°C

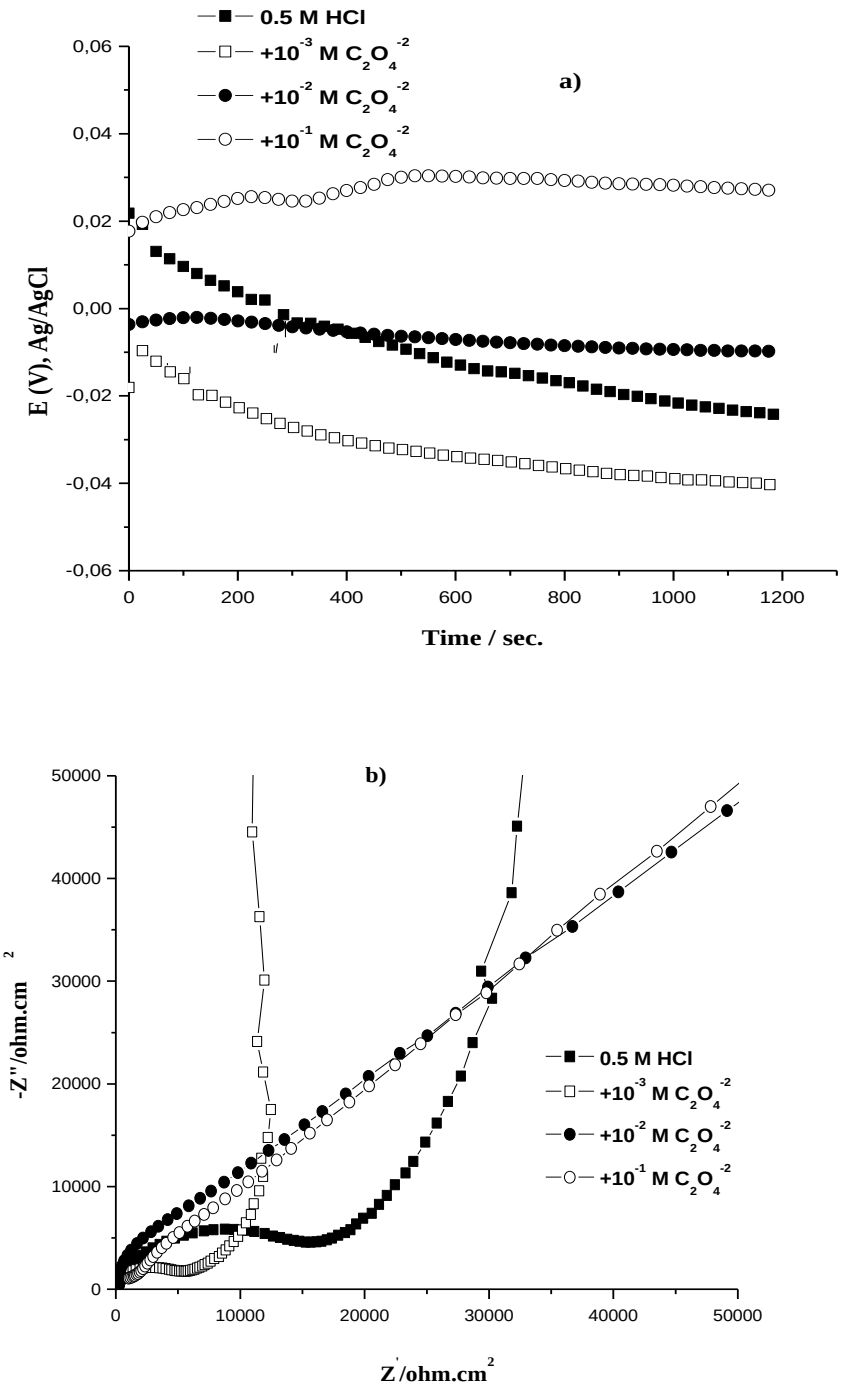

Figure 7. a) potential-time and b) impedance curves of 99.95 % purity molybdenum in 0.5 M HCl + x M $C_2O_4^{2-}$ [x: 0 (■), 10^{-3} M (□), 10^{-2} M (●) and 10^{-1} M (○)] solutions at 25°C

ISSN 2422-8702 (Online), **DOI:** 10.7176/JSTR/5-4-12
Vol.5, No.4, 2019

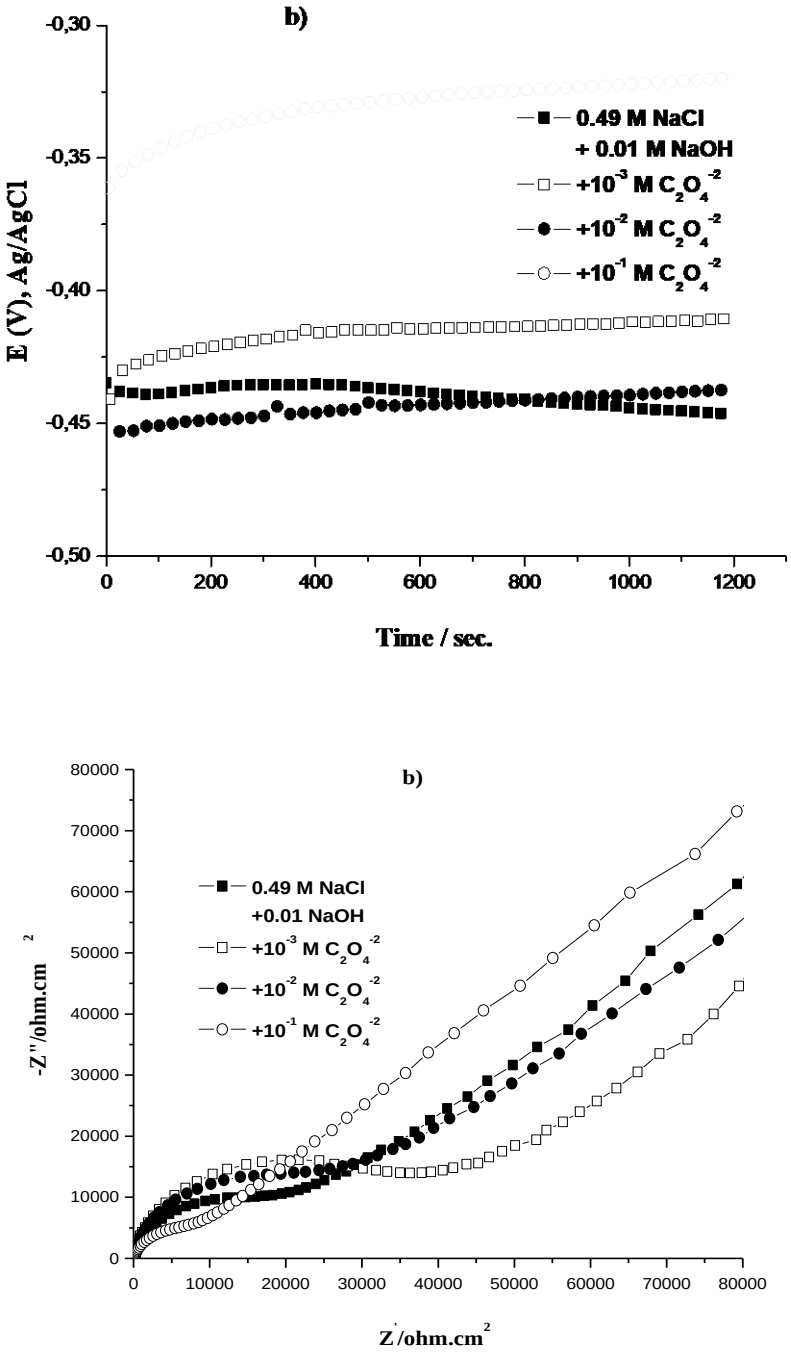

Figure 8. a) potential-time and b) impedance curves of 99.95 % purity molybdenum in 0.49 M NaCl + 0.01 M NaOH + x M $C_2O_4^{2-}$ [x: 0 (■), 10^{-3} M (□), 10^{-2} M (●) and 10^{-1} M (○)] solutions at 25°C.

From Tables 5 and 6, it is seen that the equilibrium potentials of neutral and basic solutions shift in the negative direction upon addition of $C_2O_4^{-2}$. This is an indication for cathodic inhibition of oxalate on the corrosion of molybdenum. Similar corrosion rates of molybdenum in neutral, acidic and basic solutions indicate that the metal surface has the same composition at all pH. The structure of metal surface is probably MoO_2.

Table 4. The corrosion characteristics of 99.99 % purity zinc obtained in 1 M NaCl solutions containing $C_2O_4^{2}$, WO_4^{2-}, MoO_4^{2-} and HPO_4^{2-} at 25°C

Solution	E_{corr} (V) vs. Ag/AgCl	$-b_k$ (Mv dec^{-1})	b_a (mV dec^{-1})	i_{kor} (μA/cm^2)	C_{dl} (F cm^{-2})	R_p (Ω cm^2)	% η
Blank	-1.066	334	70	34	3.78×10^{-6}	736	
$+10^{-3}$ M $C_2O_4^{-2}$	-1.068	205	52	15.2	3.32×10^{-6}	1277	55.3
$+10^{-2}$ M $C_2O_4^{-2}$	-1.080	271	46	16.4	1.07×10^{-5}	1039	51.7
$+10^{-1}$ M $C_2O_4^{-2}$	-1.194	149	353	76	3.49×10^{-5}	383	-
$+10^{-3}$ M WO_4^{-2}	-1.050	378	30	5.6	7.47×10^{-6}	2183	83.5
$+10^{-3}$ M MoO_4^{-2}	-1.022	770	35.5	7.08	6.31×10^{-6}	2118	79
$+10^{-3}$ M HPO_4^{-2}	-1.055	434	32	4.7	3.73×10^{-6}	2975	86

Table 5. The corrosion characteristics of 99.95 % purity molybdenum obtained in 0.5 M NaCl + x M $C_2O_4^{2-}$ solutions at 25°C.

X	E_{corr} (V) vs. Ag/AgCl	$-b_c$ (mV dec^{-1})	b_a (mV dec^{-1})	$R_p\times10^{+6}$ (Ω.cm^2)	C_{dl} (F/cm^2)	i_{corr} (μA/cm^2)	% η
Blank	-0.281	164.7	276.7	3.78	$6.72x10^{-5}$	0.013	
$+10^{-3}$ M $C_2O_4^{2-}$	-0.319	162.5	282.5	2.90	$2.00x10^{-4}$	0.016	-
$+10^{-2}$ M $C_2O_4^{2-}$	-0.242	220.2	216.3	7.56	$2.44x10^{-5}$	0.006	54
$+10^{-1}$ M $C_2O_4^{2-}$	-0.332	183.2	280.5	6.20	$4.48x10^{-5}$	0.008	38

Table 6. The corrosion characteristics of 99.95 % purity molybdenum obtained in 0.5 M HCl + x M $C_2O_4^{2-}$ and 0.49 M NaCl + 0.01 M NaOH + xM $C_2O_4^{2-}$ solutions at 25°C.

X	E_{corr} (V) vs. Ag/AgCl	$-b_c$ (mV dec^{-1})	b_a (mV dec^{-1})	$R_p\times10^{+6}$ (Ω.cm^2)	C_{dl} (F/cm^2)	i_{corr} (μA/cm^2)	% η
0.5 M HCl	-0.118	176	328	5.15	$6.72x10^{-5}$	0.010	
$+10^{-3}$ M $C_2O_4^{2-}$	-0.150	190	267	4.25	$1.97x10^{-4}$	0.014	-
$+10^{-2}$ M $C_2O_4^{2-}$	-0.140	193	250	4.11	$1.34x10^{-4}$	0.013	-
$+10^{-1}$ M $C_2O_4^{2-}$	-0.110	196	262	4.46	$1.12x10^{-4}$	0.011	-
0.49 M NaCl+ 0.01 M NaOH	-0.532	136	292	4.12	$5.06x10^{-5}$	0.011	-
$+10^{-3}$ M $C_2O_4^{2-}$	-0.567	191	270	10.0	$2.65x10^{-5}$	0.005	54
$+10^{-2}$ M $C_2O_4^{2-}$	-0.621	163	202	8.10	$3.84x10^{-5}$	0.008	27
$+10^{-1}$ M $C_2O_4^{2-}$	-0.513	191	252	4.66	$8.97x10^{-5}$	0.014	-

4. Conclusions

- The inhibition effect of $C_2O_4^{-2}$ is dependent on both metal composition and $C_2O_4^{-2}$ concentration.
- Metal dissolves in the form of $Zn(C_2O_4)_2^{-2}$ in presence of excess $C_2O_4^{-2}$. Therefore, oxalate is used in very few amounts or in mixed protection systems.
- MoO_4^{-2}, WO_4^{-2} and HPO_4^{-2} decrease the corrosion of zinc in neutral solutions. Inhibition rate increases with increasing metal impurity increases.
- At the high $C_2O_4^{-2}$ concentration Zn^+ ion can be form.

References

[1] J. F. Bbosich, Corrosion Prevention, Barnes and Noble Inc., New York, 1970, pp. 95-113.

[2] V. E. Carter, Metallic Corrosion for Corrosion Control, Newnes-Butterworths, London, 1977, 70-128.

[3] J. C. Scully, The Fundamentals of Corrosion, Pergamon Press, 1990, p.151.

[4] R. C. Weast, Handbook of Chemistry and Physics, 53rd edition, CRC Press, 1973, pp. 111-116.

[5] S. Maeda, M. Yamamoto, *Prog. in Org. Coat.*, 1998, 33, 83-89.

[6] K. Raeissi, M. R. Toroghinejad, *Prog. in Org. Coat.*, 2008, 48, 83-88.

[7] F. N. Grosser, R. S. Gonçalves, *Corr. Sci*., 2008, 50, 2934-2938.

[8] H. Wang, Y. Li, F. Wang, *Electro. Acta*, 2008, 54, 706-713.

[9] C. Georges, E. Rocca, P. Steinmetz, *Electro. Acta*, 2008, 53, 4839-4845.

[10] W. Li, L. Zhu, H. Liu, *Sur. and Coat. Tech.*, 2006, 201, 2505-2511.

[11] E. P. Banczek, P. R. P. Rodrigues, I. Costa, *Sur. and Coat. Tech.*, 2009, 203, 1213-1219.

[12] J. Yong-feng, Z. Hai-tao, Z. Su-min, *Trans. Non.Met. Soc. China*, 2009, 19, 1416-1422.

[13] W. Liu, F. Cao, L. Zhong, L. Zheng, B. Jia, Z. Zhang, J. Zhang, *Materials and Corr.*, 2009, 60, 795-803.

[14] G. Kılınççeker, M. Erbil, *Materials Chem.and Phy.*, 2010, 119, 30-39.

[15] S. Dönmez, A. A. Aksüt, *Protec. of Metals and Phys. Chem. of Sur.*, 2011, 47, 121-127.

[16] T. Yanardağ, A. A. Aksüt, *Asian J. of Chem*. 2011, 23, 2357-2828

[17] T. Yanardağ, A. A. Aksüt, Corrosion and Scale Inhibition (WP 1), SS 1-P-8142, Eurocorr, date of poster, September 4, Nice, France, 2009.

[18] E. Bolat, T. Yanardağ, M. Küyükoğlu, and A. A. Aksüt, *Protec. of Metals and Phys. Chem. of Sur., 2012, 48, 259–264.*

[19] M. Mouanga, P. Berçot, J. Y. Rauch, *Corr. Sci*., 2010, 52, 3984-3992.

[20] A. R. El-Sayed, H. S. Mohran, H. M. Abd el-lateef, *J. of Power Sources*, 2010, 195, 6924-6936.

[21] K. Brunelli, M. Dabala, I. Calliari, M. Magrini, *Corr. Sci*., 2005, 47, 989-901.

[22] U. C. Nwaogu, C. Blawert, N. Scharnagi, W. Dietzel, K. U. Kainer, *Corr. Sci*., 2009, 51, 2544-2556.

[23] T. Kosec, I. Milosev, B. Pihlar, *Appl. Sur. Sci*., 2007, 253, 8863-8873.

[24] J. P. Diard, B. Le Gorrec, C. Montella, *J. of Electroanalytical Chem.*, 1997, 432, 41-52.

[25] M. S. Antelman, The Encyclopedia of Chemical Electrode Potentials, *Plenum Press*, 1982, 86, 960-961.